A Comparative Performance Analysis of Interweaved and Underlay Multi-Antenna Cognitive Radio Networks

Miltiades C. Filippou, *Student Member, IEEE,* David Gesbert, *Fellow, IEEE,* and George A. Ropokis

***Abstract*—An analytical performance study is realized in this paper, focusing on multiple-input-single-output (MISO) cognitive radio (CR) systems with the aim of comparing the two most popular CR approaches, namely, the interweaved and underlay setups. The throughput-based comparison is accomplished on a fair basis, by measuring the achievable ergodic capacity of secondary communication, given an average rate-based, quality of service (QoS) constraint on primary communication. We derive closed form expressions for the outage probability at the primary user (PU), along with expressions for the ergodic capacity of the secondary user (SU). These expressions are derived as a function of key design parameters, under a rate-optimal sensing protocol for the interweaved approach, and a standard precoding and power allocation scheme for the underlay approach. By conducting this comparative study, we reveal the existence of specific regimes (in terms of primary activity, number of transmit antennas, quality of spectrum sensing), where the interweaved approach outperforms the underlay one and vice versa.**

***Index Terms*—Cognitive radio, interweaved, underlay, performance analysis, ergodic capacity.**

I. Introduction

The massive spread of current wireless services and wireless communication evolution have given rise to a great need for bandwidth with the aim of offering various services with high data rates. As a consequence, the accessible radio spectrum is becoming critically scarce, as mentioned by the Federal Communications Commission (FCC) [1]. To overcome this obstacle, the notion of cognitive radio networks (CRNs), introduced by Mitola [2], has emerged as a novel, promising technology, aiming to tackle the problem of spectrum scarcity and thus, to enhance spectral efficiency via optimizing the use of the -currently underutilized- radio spectrum [3], [4]. Up to the present, two popular CR design approaches have emerged:

(i) *Underlay* CRNs, where a primary service provider allows the reuse of its spectral resources by an unlicensed secondary system, provided that a specified, *maximum tolerated* interference level generated by the secondary transmitter will not be violated and

(ii) *Interweaved* CRNs, in which the secondary network (either the transmitter or the receiver) senses the frequency spectrum and decides to transmit whenever the spectrum is not occupied by primary transmissions.

Quite surprisingly and to the best of our knowledge, little effort has been made to compare such designs, based on a meaningful, fair, and even less so in an analytical manner. Indeed, the philosophies behind each CRN approach seem incompatible at first glance. The underlay approach seems to be typically reserved for applications with only loose QoS guarantees at the legacy (primary) network. On the other hand, the interweaved design is expected to offer a near-zero disturbance at the PU, hence seems to offer hard QoS guarantees.

Upon closer inspection, it is clear that the QoS achieved at the PU under the interweaved approach, strongly depends on the sensing capability at the secondary side. Sensing imperfections due to a number of factors such as channel fading, shadowing, or noise give rise to miss-detection events, which, in turn, lead to outage events at the PU due to unintentional, harmful interference towards it [5]. Arguably, a strictly conservative spectrum sensing design would ensure that near zero interference is generated at the PU. However, this strategy would inevitably lead to a wasteful spending of secondary communication resources, as it is practically difficult to sense and communicate at the same time for the secondary system. Therefore, a low outage probability at the PU, induced by a high accuracy sensing goes at the cost of data rate for the SU. An interesting question lies in whether a similar trade-off can be explored for the underlay scenario and ultimately compared with that obtained in the interweaved case. Our answer is positive.

In the underlay case, a low outage probability at the PU is maintained through a suitable power control policy at the secondary transmitter, augmented with a possible beamforming (BF) solution, when the latter is equipped with several antennas. More generally, a specific precoding and power allocation policy will lead to a specific point in the so-called outage (at PU) versus average rate (at SU) region.

The above observations motivate us to compare the throughput performance of the interweaved and underlay CRN approaches on an equal footing. More concretely, our aim is to compare the two CRN approaches with respect to the achievable SU ergodic rate, subject to a common outage

This work was supported by the French national ANR-VERSO funded project LICORNE. Dr. Ropokis was funded by the MIMOCORD project. The project is implemented within the framework of the Action “Supporting Postdoctoral Researchers” of the Operational Program “Education and Lifelong Learning” (Action’s Beneficiary: General Secretariat for Research and Technology), and is co-financed by the European Social Fund (ESF) and the Greek State.

M.C. Filippou and D. Gesbert are with EURECOM, 06410 Biot France (e-mail: filippou@eurecom.fr, gesbert@eurecom.fr).

G.A. Ropokis is with EURECOM, 06410 Biot France and with Computer Technology Institute and Press “Diophantus”, 26500, Rio-Patras, Greece (e-mail: ropokis@eurecom.fr).

probability at the PU. Marking the difference with prior CRN work, where the main quality indicator at the PU is in terms of the interference power not exceeding an arbitrary threshold, we use a definition of outage with a greater relevance to the actual PU quality-of-experience. Here, an outage event is declared when the *rate* at the PU falls below a given threshold, *whether due to interference or a fading event in its own channel*. The intuition is that a PU with a higher quality channel is likely to tolerate more interference, which ought to benefit the data rate of the secondary system.

In this context, some interesting prior work is noteworthy. In [6], the throughput potential of different CR techniques has been investigated from an information theoretical point of view. Nevertheless, no expressions describing the achievable ergodic capacity of the SU or the outage probability of the primary system are given considering a fading environment. Also, in [7], although expressions for the instantaneous rate of the SU are given, the assumption of perfect spectrum sensing is adopted, which is rather unrealistic within the CRN context. Furthermore, in [8], [9] and [10] novel spectrum sharing models are proposed, either mixed ones or variants of the interweaved model, though no explicit performance comparison of the two mentioned CRN approaches is presented. Additionally, works such as [11]–[17] focus on the derivation of either approximations or closed form expressions for the ergodic capacity of SU as well as for the outage probability of the primary system. Yet, no performance comparison between interweaved and underlay CRN approaches is illustrated in these works.

In this paper, both the interweaved and underlay CRN approaches are investigated with respect to a MISO CRN and compared with reference to the ergodic capacity of the SU for a target outage probability of the PU, as well as for various primary communication activity profiles and transmit antenna numbers. It is worth noticing that in [18] a performance-based comparison was conducted with respect to single-input-single-output (SISO) CRNs, which differs from this work. More concretely, our contributions are the following:

- Closed form expressions for the outage probability of primary communication, regarding both MISO interweaved and underlay CRN approaches, are derived.
- Expressions for the ergodic capacity of the SU are derived with respect to both MISO CRN approaches.
- Rate-optimal values of each CR system's generic design parameters are found, corresponding to a common outage probability at the PU.
- The optimal SU ergodic throughput levels of the two CRN approaches are finally compared, under a target outage level of the PU, for various primary communication activity profiles and transmit antenna numbers. It is shown that the performance comparison results are driven by a set of key system parameters such as the number of transmit antennas, the activity profile of the primary system, as well as the spectrum sensing protocol design parameters.

Throughout the paper, the following notations are adopted: all boldface letters indicate vectors (lower case) or matrices (upper case). Superscript $(\cdot)^H$ stands for Hermitian transpose and $\mathbb{E}\{\cdot\}$ symbolizes the expectation operator. $\mathcal{P}(A)$ denotes the probability of event A and $\|\cdot\|$ is the Euclidean norm. The identity matrix of dimension $n \times n$ is denoted by $\mathbf{I}_n$. For a random vector $\mathbf{x}$, $\mathbf{x} \sim \mathcal{CN}(\boldsymbol{\mu}, \boldsymbol{\Sigma})$ denotes that $\mathbf{x}$ follows a circularly symmetric complex Gaussian (CSCG) distribution with mean $\boldsymbol{\mu}$ and covariance matrix $\boldsymbol{\Sigma}$. Also, $E_1(\cdot)$ represents the exponential integral function, which is defined in [19, 5.1.1], whereas $\mathcal{Q}(\cdot)$ stands for the complementary Gaussian distribution function [20, 4.1]. Additionally, $\Gamma(n)$, where $n \in \mathbb{N}$, denotes Gamma function defined in [19, 6.1.6], whereas $\gamma(n,x)$ and $\Gamma(n,x)$ denote the lower and upper incomplete Gamma functions, defined in [19, 6.5.2] and in [19, 6.5.3], respectively.

II. System and Channel Model

The system under investigation, which is illustrated in Fig. 1 consists of a MISO primary system, comprising of a base station (BS), BS_p, equipped with M antennas, as well as its assigned PU, UE_p. Focusing on downlink communication, the primary system is willing to share its resources with a MISO secondary system consisting of a BS, BS_s, also equipped with M antennas, along with its assigned SU, UE_s. It is assumed that $1 \times M$ channels $\mathbf{h}_{ij}$, $i,j \in \{p,s\}$ between BS_i and user UE_j as well as channel $\mathbf{h}_{00}$ between BS_p and one of the antennas at BS_s (which will be later devoted to spectrum sensing within the interweaved CRN context), are Rayleigh fading ones, i.e., $\mathbf{h}_{ij} \sim \mathcal{CN}(\mathbf{0}, \sigma_{ij}^2 \mathbf{I}_M)$ $i,j \in \{p,s\}$ and $\mathbf{h}_{00} \sim \mathcal{CN}(\mathbf{0}, \sigma_{00}^2 \mathbf{I}_M)$.

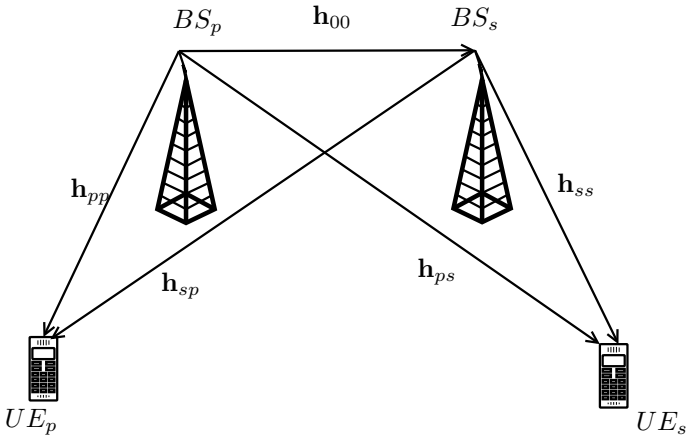

Fig. 1. MISO CRN - System topology.

In the following two sections, closed form expressions for the outage probability of primary communication as well as expressions for the ergodic capacity of the SU, will be derived for both the interweaved and underlay CRN approach. It is assumed that BS_p can perfectly estimate channel $\mathbf{h}_{pp}$ and BS_s has a perfect estimate of channel vector $\mathbf{h}_{ss}$, while it has statistical knowledge of channel $\mathbf{h}_{pp}$.

III. Performance Analysis of the Interweaved Approach

A. General model

We consider first the interweaved approach, as it is shown in Fig. 2, where each medium access control (MAC) frame

is assumed to have a duration of T time units, including a subframe dedicated to *spectrum sensing*, which lasts for $\tau < T$ time units. The rest of the frame is dedicated to data transmission. Moreover, during each sensing phase, BS_s receives $N = \tau f_s$ samples, where f_s is the sampling frequency of the received signal. It is also assumed that during sensing, BS_s is kept silent and all instantaneous channels remain constant within a MAC frame. Note that we assume here that the spectrum sensing process takes place at the secondary transmitter as opposed to e.g., at the receiving terminal side, thereby by passing the need for a dedicated sensing feedback channel.

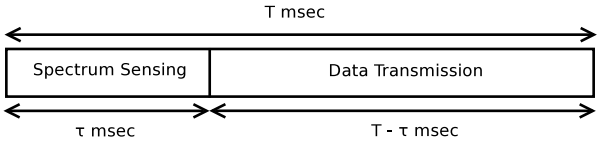

Fig. 2. MAC frame structure.

Energy detection is applied as it is a popular and easily applicable spectrum sensing scheme [21]. At the n-th, $n = 1, 2, \ldots, N$ time instant, the binary hypothesis test for spectrum sensing is expressed as

$$y_s[n] = \begin{cases} z[n], & \text{if } \mathcal{H}_0 \\ \mathbf{h}_{00}\mathbf{w}_p s_p[n] + z[n], & \text{if } \mathcal{H}_1, \end{cases} \tag{1}$$

where additive noise $z[n]$ is a CSCG, independent, identically distributed (i.i.d) process with $z[n] \sim \mathcal{CN}(0, N_0)$, P_p is a fixed power level at BS_p and the information symbol $s_p[n]$ is selected from a CSCG codebook, i.e., $s_p[n] \sim \mathcal{CN}(0, 1)$ and is independent of $z[n]$. Vector $\mathbf{w}_p \in \mathbb{C}^{M\times 1}$ is the applied BF vector at BS_p. We assume that when the primary system is in transmission mode, Maximal Ratio Combining (MRC) BF with full power is applied at BS_p, since the goal of the primary transmitter is to maximize the rate of the PU. Similarly, when the secondary system decides to transmit, also full power MRC BF is applied at BS_s. Hence, we obtain the following expressions for the unit-norm beamformers (BFs):

$$\mathbf{w}_p = \sqrt{P_p}\frac{\mathbf{h}_{pp}^H}{\|\mathbf{h}_{pp}\|} = \sqrt{P_p}\tilde{\mathbf{h}}_{pp}^H \tag{2}$$

and

$$\mathbf{w}_s^{int} = \sqrt{P_s}\frac{\mathbf{h}_{ss}^H}{\|\mathbf{h}_{ss}\|} = \sqrt{P_s}\tilde{\mathbf{h}}_{ss}^H, \tag{3}$$

respectively.

As it can be easily derived, signal $s[n] = \mathbf{h}_{00}\mathbf{w}_p s_p[n]$, for a fixed channel $\mathbf{h}_{00}$, will have a variance of $\sigma_s^2 = \mathbb{E}\{|s[n]|^2\} = P_p|\mathbf{h}_{00}\tilde{\mathbf{h}}_{pp}^H|^2$.

For a fixed sensing time, τ, along with a fixed energy detection threshold, ϵ, by applying central limit theorem, the probability of false alarm, $\mathcal{P}_{fa}$, as well as the corresponding probability of detection, $\mathcal{P}_d$, can be derived, with reference to a specific MAC frame, by applying [22, Proposition 1, Proposition 2]. The above probabilities can then be written as

$$\mathcal{P}_{fa} = \mathcal{Q}\Big(\sqrt{N}\Big(\frac{\epsilon}{N_0} - 1\Big)\Big), \quad \mathcal{P}_d = \mathcal{Q}\Big(\frac{\epsilon - \mu_1}{\sigma_1}\Big), \tag{4}$$

where $\mu_1 = \sigma_s^2 + N_0 = P_p|\mathbf{h}_{00}\tilde{\mathbf{h}}_{pp}^H|^2 + N_0$ and $\sigma_1^2 = \frac{N_0^2}{N}\left(\frac{P_p|\mathbf{h}_{00}\tilde{\mathbf{h}}_{pp}^H|^2}{N_0} + 1\right)^2$.

The average detection probability with reference to random variable $\beta_{00} = |\mathbf{h}_{00}\tilde{\mathbf{h}}_{pp}^H|^2$, is given by

$$\mathcal{P}_d^{avg} = \int_0^\infty \mathcal{P}_d(\beta_{00}) f_{\beta_{00}}(\beta_{00}) d\beta_{00}. \tag{5}$$

Although we need an expression for $\mathcal{P}_d^{avg}$ as a function of τ and ϵ so as to maximize the rate of the SU over these two parameters, doing this proves to be difficult due to the lack of a closed form expression of (5). Instead, we now resort to a bounding argument to solve this problem approximately. Note that the accuracy of this bounding strategy is justified by our simulations in section VI.

To obtain a bound on (5), we use the fact that the detection probability in (4), although neither strictly concave nor convex as a function of β_{00}, is concave in the region of interest for β_{00} (the region corresponding to high detection probability). Therefore, the applied bound is the following

$$\mathcal{P}_{d,B} = \mathcal{Q}\Big(\sqrt{N}\Big(\frac{\epsilon}{P_p\sigma_{00}^2 + N_0} - 1\Big)\Big). \tag{6}$$

Regarding the average false alarm probability, it remains the same under any fading channel, for given τ and ϵ, since $\mathcal{P}_{fa}$ is considered for the case where only noise is present, thus

$$\mathcal{P}_{fa}^{avg} = \mathcal{P}_{fa}. \tag{7}$$

B. Outage probability of primary communication

Although the interference power at the PU is used as a quality indicator in much of the CRN literature, we point out that when it comes to primary data rate, it is the signal-to-interference plus noise ratio (SINR) at the PU which rather governs performance. To reflect this, we assume an outage at the PU when, given that the primary network is active, the SINR of the PU is below a predefined threshold, γ_0. This can occur in two cases:

1) when BS_s fails to sense primary activity (missed detection), potentially resulting to a PU SINR that is less than γ_0 or
2) when the secondary system has correctly detected the presence of a primary signal and remains silent for the rest of the MAC frame. Yet, the desired signal received at the PU is fading, so that the SINR falls below the threshold γ_0.

In the proposition that follows, a closed form expression of PU outage probability is given.

Proposition 1. The outage probability of primary communication for a MISO interweaved CRN is given by the following expression

$$\mathcal{P}_{out}^{int} = (1-\mathcal{P}_d)\mathcal{P}_1 + \mathcal{P}_d\mathcal{P}_2, \tag{8}$$

where

$$\mathcal{P}_1 = 1 - \frac{e^{-\gamma_0 N_0 B\left(\frac{1}{\lambda_{X_1}}-\tilde{\mu}\right)}}{\lambda_{X_2}\lambda_{X_1}^M}\sum_{k=0}^{M-1}\frac{\lambda_{X_1}^{M-k}}{k!\tilde{\mu}^{k+1}}\Gamma(k+1,\gamma_0 N_0 B\tilde{\mu}), \tag{9a}$$

$$\mathcal{P}_2 = \frac{\gamma\left(M, \frac{\gamma_0 N_0 B}{\lambda_{X_1}}\right)}{\Gamma(M)}, \tag{9b}$$

with $\lambda_{X_1} = P_p\sigma_{pp}^2$, $\lambda_{X_2} = \gamma_0 P_s\sigma_{sp}^2$, $\tilde{\mu} = \frac{1}{\lambda_{X_1}} + \frac{1}{\lambda_{X_2}}$ and P_s stands for the maximum instantaneous available power at the secondary transmitter.

Proof. See Appendix A. □

C. Ergodic capacity of secondary communication

By applying the upper bound for the average detection probability, $\mathcal{P}_{d,B}$, the ergodic capacity of the SU will have a lower bound, that is given as

$$\mathbb{E}\{R_s^{int}\} \geq \frac{(T-\tau)}{T}\Bigg(\mathcal{P}(\mathcal{H}_0)(1-\mathcal{P}_{fa})B\mathbb{E}\Big\{\underbrace{\log_2\left(1+\frac{P_s\|\mathbf{h}_{ss}\|^2}{N_0B}\right)}_{\mathcal{A}_1}\Big\} + \mathcal{P}(\mathcal{H}_1)(1-\mathcal{P}_{d,B})B\mathbb{E}\Big\{\underbrace{\log_2\left(1+\frac{P_s\|\mathbf{h}_{ss}\|^2}{N_0B+P_p|\mathbf{h}_{ps}\tilde{\mathbf{h}}_{pp}^H|^2}\right)}_{\mathcal{A}_2}\Big\}\Bigg). \tag{10}$$

We first focus on computing expectation $\mathbb{E}\{\mathcal{A}_1\}$. Random variable $Y_1 = P_s\|\mathbf{h}_{ss}\|^2$ is gamma distributed with PDF $f_{Y_1}(y_1) = \frac{y_1^{M-1}e^{-\frac{y_1}{\lambda_{Y_1}}}}{\Gamma(M)\lambda_{Y_1}^M}$, where $\lambda_{Y_1} = P_s\sigma_{ss}^2$. Hence, using [23, 4.337.5], we have

$$\mathbb{E}\{\mathcal{A}_1\} = \frac{1}{\ln(2)}\sum_{j=0}^{M-1}\frac{1}{(M-j-1)!}\Bigg(\frac{(-1)^{M-j-3}}{\left(\frac{\lambda_{Y_1}}{N_0B}\right)^{M-j-1}}e^{\frac{N_0B}{\lambda_{Y_1}}}\times E_1\left(\frac{N_0B}{\lambda_{Y_1}}\right) + \sum_{k=1}^{M-j-1}(k-1)!\left(\frac{-N_0B}{\lambda_{Y_1}}\right)^{M-j-k-1}\Bigg). \tag{11}$$

For the expectation appearing in the second term of (10), one obtains

$$\mathbb{E}\{\mathcal{A}_2\} = \frac{1}{\ln(2)}\mathbb{E}\left\{\ln\left(1+\frac{Y_1}{N_0B+Y_2}\right)\right\} = \frac{1}{\ln(2)}\Bigg(\underbrace{\int_0^\infty f_{Y_1}(y_1)\int_0^\infty \ln(N_0B+y_1+y_2)f_{Y_2}(y_2)dy_2dy_1}_{\mathcal{J}_1} - \underbrace{\int_0^\infty f_{Y_1}(y_1)\int_0^\infty \ln(N_0B+y_2)f_{Y_2}(y_2)dy_2dy_1}_{\mathcal{J}_2}\Bigg). \tag{12}$$

Random variable $Y_2 = P_p|\mathbf{h}_{ps}\tilde{\mathbf{h}}_{pp}^H|^2$ is independent of Y_1 and exponentially distributed with PDF $f_{Y_2}(y_2) = \frac{1}{\lambda_{Y_2}}e^{\frac{-y_2}{\lambda_{Y_2}}}$, where $\lambda_{Y_2} = P_p\sigma_{ps}^2$. The derivation of double integral $\mathcal{J}_1$ gives

$$\mathcal{J}_1 = \mathcal{J}_{1,1} + \mathcal{J}_{1,2}, \tag{13}$$

where by exploiting [23, 4.337.5]

$$\mathcal{J}_{1,1} = \ln(N_0B) + \sum_{j=0}^{M-1}\frac{1}{(M-j-1)!}\Bigg(\frac{(-1)^{M-j-3}}{\left(\frac{\lambda_{Y_1}}{N_0B}\right)^{M-j-1}}e^{\frac{N_0B}{\lambda_{Y_1}}}\times E_1\left(\frac{N_0B}{\lambda_{Y_1}}\right) + \sum_{k=1}^{M-j-1}(k-1)!\left(\frac{-N_0B}{\lambda_{Y_1}}\right)^{M-j-k-1}\Bigg), \tag{14}$$

and

$$\mathcal{J}_{1,2} = \frac{1}{\Gamma(M)}\int_0^\infty e^{-u}u^{M-1}e^{\frac{N_0B+\lambda_{Y_1}u}{\lambda_{Y_2}}}E_1\left(\frac{N_0B+\lambda_{Y_1}u}{\lambda_{Y_2}}\right)du. \tag{15}$$

Since a closed form expression of the last integral cannot be derived, numerical integration can be applied by employing the well-known Laguerre quadrature rules [19, 25.4.45].

Double integral $\mathcal{J}_2$ can be found in closed form by applying [23, 3.351.3], therefore, the following expression is obtained

$$\mathcal{J}_2 = \ln(N_0B) + e^{\frac{N_0B}{\lambda_{Y_2}}}E_1\left(\frac{N_0B}{\lambda_{Y_2}}\right). \tag{16}$$

In the following section, a closed form expression for the outage probability of the PU, as well as an expression for the ergodic capacity of the SU will be derived considering an underlay CRN. Both cases of MRC as well as zero-forcing (ZF) BF at the secondary transmitter, will be examined.

IV. Performance Analysis of the Underlay Approach

A. Power and BF policies

In the underlay approach, the secondary transmitter is in principle always active. It maintains the prescribed PU outage probability level by suitably adjusting its transmit power and beam vector. To do so, note that the secondary transmitter requires *some* knowledge about interference channel $\mathbf{h}_{sp}$, which is otherwise not needed in the interweaved scenario. This information is assumed to be obtained via feedback in Frequency Division Duplex (FDD), or reciprocity in Time Division Duplex (TDD) scenarios.

Our channel state information at the transmitter (CSIT) model, nevertheless, leaves the direct primary channel, $\mathbf{h}_{pp}$, unknown at the secondary transmitter, hence the power policy is designed to depend only on the interference channel gain and on the *statistics* of channel $\mathbf{h}_{pp}$. In such conditions, the secondary transmit power is adapted to meet an *average* outage constraint at the PU.

When it comes to BF, we will focus on the MRC strategy, identical to the interweaved case. At the end of this section, we also compare with a ZF strategy, for reference. However, this would require full interference channel knowledge.

B. Power policy at the secondary link under MRC

In order to meet an average outage level at the PU, the secondary transmitter adapts its power, $P_{s,MRC}^{und}$ in order to meet a certain interference level, $\mathcal{I}$. The optimal interference level is not known a priori but it can be optimized on the basis of the instantaneous interference gain and the statistics of channel $\mathbf{h}_{pp}$. Let $\mathbf{w}_{s,MRC}^{und} = \sqrt{P_{s,MRC}^{und}}\tilde{\mathbf{h}}_{ss}^{H}$ be the transmission BF policy applied by BS_s. Power $P_{s,MRC}^{und}$ can vary from zero to a maximum instantaneous value, P_s. The maximum instantaneous power level is taken to be equal to the one considered in the interweaved approach in order to conduct a fair comparison from a power consumption perspective. Therefore, an MRC BF policy with truncated power will be applied in this case at BS_s. The truncated power policy is the following

$$P_{s,MRC}^{und} = \begin{cases} \frac{\mathcal{I}}{|\mathbf{h}_{sp}\tilde{\mathbf{h}}_{ss}^{H}|^2}, & \text{if } \frac{\mathcal{I}}{|\mathbf{h}_{sp}\tilde{\mathbf{h}}_{ss}^{H}|^2} < P_s \\ P_s, & \text{if } \frac{\mathcal{I}}{|\mathbf{h}_{sp}\tilde{\mathbf{h}}_{ss}^{H}|^2} \geq P_s. \end{cases} \tag{17}$$

In what follows, a closed form expression for the outage probability of primary communication, as well as an approximation of the achievable ergodic capacity of the SU, will be derived, focusing on the underlay CRN approach, when MRC BF is used at the secondary transmitter.

1) Outage probability of primary communication: The primary system is in outage when the instantaneous SINR of the PU is below threshold γ_0. In the following proposition, a closed form expression of the outage probability of the PU, for a given interference threshold, $\mathcal{I}$, is given.

Proposition 2. The outage probability of primary communication for a MISO underlay CRN, where MRC-based BF, as well as a truncated power allocation policy, are applied at BS_s, is given by

$$\mathcal{P}_{out,MRC}^{und} = \frac{\gamma\big(M, \frac{\gamma_0 N_0 B}{P_p\sigma_{pp}^2}\big)}{\Gamma(M)} + \frac{e^{\frac{N_0 B}{P_s\sigma_{sp}^2}}}{\Gamma(M)}\left(\frac{P_p\sigma_{pp}^2}{\gamma_0 P_s\sigma_{sp}^2}+1\right)^{-M} \times \left(\Gamma\left(M, \frac{N_0 B}{P_s\sigma_{sp}^2} + \frac{\gamma_0 N_0 B}{P_p\sigma_{pp}^2}\right) - \Gamma\left(M, \frac{N_0 B+\mathcal{I}}{P_s\sigma_{sp}^2} + \frac{\gamma_0(N_0 B+\mathcal{I})}{P_p\sigma_{pp}^2}\right)\right). \tag{18}$$

Proof. See Appendix B. □

2) Ergodic capacity of secondary communication: Following the BF as well as the truncated power transmission policy described in (17), the expression describing the ergodic rate of the SU will be the one that follows

$$\mathbb{E}\{R_{s,MRC}^{und}\} = \mathcal{P}(\mathcal{H}_0)B\mathbb{E}\Big\{\underbrace{\log_2\left(1+\frac{P_{s,MRC}^{und}\|\mathbf{h}_{ss}\|^2}{N_0 B}\right)}_{\mathcal{B}_1}\Big\} + \mathcal{P}(\mathcal{H}_1)B\mathbb{E}\Big\{\underbrace{\log_2\left(1+\frac{P_{s,MRC}^{und}\|\mathbf{h}_{ss}\|^2}{N_0 B+P_p|\mathbf{h}_{ps}\tilde{\mathbf{h}}_{pp}^{H}|^2}\right)}_{\mathcal{B}_2}\Big\}. \tag{19}$$

a) Deriving expectation $\mathbb{E}\{\mathcal{B}_1\}$: Expectation $\mathbb{E}\{\mathcal{B}_1\}$, appearing in the first term of (19), is given by the following expression

$$\mathbb{E}\{\mathcal{B}_1\} = \frac{1}{\ln(2)}\Bigg(\mathbb{E}\Big\{\underbrace{\ln\left(1+\frac{\mathcal{I}\|\mathbf{h}_{ss}\|^2}{N_0 B|\mathbf{h}_{sp}\tilde{\mathbf{h}}_{ss}^{H}|^2}\right)}_{\mathcal{C}_1}\Big\} + \mathcal{P}\Big\{\frac{\mathcal{I}}{|\mathbf{h}_{sp}\tilde{\mathbf{h}}_{ss}^{H}|^2}\geq P_s\Big\}\mathbb{E}\Big\{\underbrace{\ln\left(1+\frac{P_s\|\mathbf{h}_{ss}\|^2}{N_0 B}\right)}_{\mathcal{C}_2}\Big\}\Bigg), \tag{20}$$

where $\mathcal{P}\Big\{\frac{\mathcal{I}}{|\mathbf{h}_{sp}\tilde{\mathbf{h}}_{ss}^{H}|^2}\geq P_s\Big\} = 1-e^{-\frac{\mathcal{I}}{P_s\sigma_{sp}^2}}$.

Gamma distributed random variable $Z_1 = \|\mathbf{h}_{ss}\|^2$ and exponentially distributed random variable $Z_2 = |\mathbf{h}_{sp}\tilde{\mathbf{h}}_{ss}^{H}|^2$ are independent, since channel vectors $\mathbf{h}_{ss}$ and $\mathbf{h}_{sp}$ are considered independent and norm $\|\mathbf{h}_{ss}\|$ is independent of direction $\tilde{\mathbf{h}}_{ss}$ [24, A.1.3]. As a consequence, we obtain the following expression for expectation $\mathbb{E}\{\mathcal{C}_1\}$

$$\begin{aligned}\mathbb{E}\{\mathcal{C}_1\} &= \int_0^\infty\int_{\frac{\mathcal{I}}{P_s}}^\infty \ln\left(1+\frac{Iz_1}{N_0 B z_2}\right)f_{Z_1,Z_2}(z_1,z_2)dz_2dz_1 \\ &= \underbrace{\int_0^\infty f_{Z_1}(z_1)\int_{\frac{\mathcal{I}}{P_s}}^\infty \ln(\mathcal{I}z_1+N_0 B z_2)f_{Z_2}(z_2)dz_2dz_1}_{\mathcal{K}_1} \\ &\quad - \underbrace{\int_0^\infty f_{Z_1}(z_1)\int_{\frac{\mathcal{I}}{P_s}}^\infty \ln(N_0 B z_2)f_{Z_2}(z_2)dz_2dz_1}_{\mathcal{K}_2}.\end{aligned} \tag{21}$$

For double integral $\mathcal{K}_1$, by applying [23, 3.352.2] we obtain

$$\mathcal{K}_1 = \mathcal{K}_{1,1} + \mathcal{K}_{1,2}, \tag{22}$$

where, by using expressions [23, 3.351.3] and [23, 4.337.5] we have

$$\mathcal{K}_{1,1} = e^{\frac{-\mathcal{I}}{P_s\sigma_{sp}^2}}\left(\ln\left(\frac{N_0 B\mathcal{I}}{P_s}\right)+\sum_{j=0}^{M-1}\frac{1}{(M-j-1)!}\left(\frac{(-1)^{M-j-3}}{\left(\frac{P_s\sigma_{ss}^2}{N_0 B}\right)^{M-j-1}} \times e^{\frac{N_0 B}{P_s\sigma_{ss}^2}}E_1\left(\frac{N_0 B}{P_s\sigma_{ss}^2}\right)+\sum_{k=1}^{M-j-1}(k-1)!\left(\frac{-N_0 B}{P_s\sigma_{ss}^2}\right)^{M-j-k-1}\right)\right). \tag{23}$$

Term $\mathcal{K}_{1,2}$ is given by the following expression

$$\mathcal{K}_{1,2} = \frac{1}{\Gamma(M)}\int_0^\infty e^{-u}u^{M-1}e^{u\frac{\mathcal{I}\sigma_{ss}^2}{\sigma_{sp}^2 N_0 B}}E_1\left(\frac{\mathcal{I}}{P_s\sigma_{sp}^2}+u\frac{\mathcal{I}\sigma_{ss}^2}{\sigma_{sp}^2 N_0 B}\right)du, \tag{24}$$

which can be also computed by employing Laguerre quadrature rules. Double integral $\mathcal{K}_2$ is derived by using integration by parts and applying [23, 3.352.2], thus, giving

$$\mathcal{K}_2 = \ln\left(\frac{N_0 B\mathcal{I}}{P_s}\right)e^{\frac{-\mathcal{I}}{P_s\sigma_{sp}^2}} + E_1\left(\frac{\mathcal{I}}{P_s\sigma_{sp}^2}\right). \tag{25}$$

Finally, by using [23, 4.337.5], expectation $\mathbb{E}\{\mathcal{C}_2\}$ is given by the following expression

$$\mathbb{E}\{\mathcal{C}_2\}=\sum_{j=0}^{M-1}\frac{1}{(M-j-1)!}\Bigg(\frac{(-1)^{M-j-3}}{\left(\frac{P_s\sigma_{ss}^2}{N_0B}\right)^{M-j-1}}e^{\frac{N_0B}{P_s\sigma_{ss}^2}}\times E_1\Big(\frac{N_0B}{P_s\sigma_{ss}^2}\Big)+\sum_{k=1}^{M-j-1}(k-1)!\Big(\frac{-N_0B}{P_s\sigma_{ss}^2}\Big)^{M-j-k-1}\Bigg). \tag{26}$$

b) Deriving expectation $\mathbb{E}\{\mathcal{B}_2\}$: In a similar way, expectation $\mathbb{E}\{\mathcal{B}_2\}$, appearing in the second term of (19), is given by the following expression

$$\mathbb{E}\{\mathcal{B}_2\}=\frac{1}{\ln(2)}\Bigg(\underbrace{\mathbb{E}\Big\{\ln\Big(1+\frac{\mathcal{I}\|\mathbf{h}_{ss}\|^2}{|\mathbf{h}_{sp}\tilde{\mathbf{h}}_{ss}^H|^2(N_0B+P_p|\mathbf{h}_{ps}\tilde{\mathbf{h}}_{pp}^H|^2)}\Big)\Big\}}_{\mathcal{D}_1}+\mathcal{P}\Big\{\frac{\mathcal{I}}{|\mathbf{h}_{sp}\tilde{\mathbf{h}}_{ss}^H|^2}\geq P_s\Big\}\underbrace{\mathbb{E}\Big\{\ln\Big(1+\frac{P_s\|\mathbf{h}_{ss}\|^2}{N_0B+P_p|\mathbf{h}_{ps}\tilde{\mathbf{h}}_{pp}^H|^2}\Big)\Big\}}_{\mathcal{D}_2}\Bigg). \tag{27}$$

Random variables Z_1, Z_2 as well as exponentially distributed random variable $Z_3=|\mathbf{h}_{ps}\tilde{\mathbf{h}}_{pp}^H|^2$ are independent, thus, one obtains for expectation $\mathbb{E}\{\mathcal{D}_1\}$ the following expression

$$\begin{aligned}\mathbb{E}\{\mathcal{D}_1\}&=\int_0^\infty\int_0^\infty\int_{\frac{\mathcal{I}}{P_s}}^\infty\ln\Big(1+\frac{\mathcal{I}z_1}{z_2(N_0B+P_pz_3)}\Big)f_{Z_1,Z_2,Z_3}(z_1,z_2,z_3)dz_2dz_3dz_1\\&=\underbrace{\int_0^\infty f_{Z_1}(z_1)\int_0^\infty f_{Z_3}(z_3)\int_{\frac{\mathcal{I}}{P_s}}^\infty\ln(\mathcal{I}z_1+z_2(N_0B+P_pz_3))f_{Z_2}(z_2)dz_2dz_3dz_1}_{\mathcal{L}_1}\\&\quad\underbrace{-\int_0^\infty f_{Z_1}(z_1)\int_0^\infty f_{Z_3}(z_3)\int_{\frac{\mathcal{I}}{P_s}}^\infty\ln(z_2(N_0B+P_pz_3))f_{Z_2}(z_2)dz_2dz_3dz_1}_{\mathcal{L}_2},\end{aligned} \tag{28}$$

where $f_{Z_1,Z_2,Z_3}(z_1,z_2,z_3)$ is the joint PDF of random variables Z_1, Z_2 and Z_3.

Focusing on multiple integral $\mathcal{L}_1$, by making use of [23, 3.352.2], we obtain

$$\mathcal{L}_1=\mathcal{L}_{1,1,1}+\mathcal{L}_{1,1,2}+\mathcal{L}_{1,2}, \tag{29}$$

where, for the first term of (29), by using [23, 4.337.5], it can be shown that $\mathcal{L}_{1,1,1}=\mathcal{K}_{1,1}$. The derivation of term $\mathcal{L}_{1,1,2}$, leads to the following expression

$$\mathcal{L}_{1,1,2}=\frac{e^{\frac{-\mathcal{I}}{P_s\sigma_{sp}^2}}}{\Gamma(M)}\int_0^\infty e^{-u}u^{M-1}e^{\frac{N_0B+P_s\sigma_{ss}^2u}{P_p\sigma_{ps}^2}}E_1\Big(\frac{N_0B+P_s\sigma_{ss}^2u}{P_p\sigma_{ps}^2}\Big)du, \tag{30}$$

which can be computed by applying [19, 25.4.45].

Term $\mathcal{L}_{1,2}$ is given by the following expression

$$\mathcal{L}_{1,2}=\frac{1}{\Gamma(M)}\int_0^\infty e^{-u_1}\int_0^\infty e^{-u_3}u_1^{M-1}e^{\frac{\mathcal{I}\sigma_{ss}^2u_1}{\sigma_{sp}^2(N_0B+P_p\sigma_{ps}^2u_3)}}\times E_1\Big(\frac{\mathcal{I}}{P_s\sigma_{sp}^2}+\frac{\mathcal{I}\sigma_{ss}^2u_1}{\sigma_{sp}^2(N_0B+P_p\sigma_{ps}^2u_3)}\Big)du_3du_1. \tag{31}$$

Since a closed form expression of the latter double integral cannot be derived, two dimensional numerical integration can be applied by employing twice, one for each dimension, the Laguerre quadrature rules [19, 25.4.45].

Moreover, one can compute multiple integral $\mathcal{L}_2$ by using [23, 3.352.2], giving

$$\mathcal{L}_2=e^{\frac{-\mathcal{I}}{P_s\sigma_{sp}^2}}\Bigg(\ln\Big(\frac{N_0B\mathcal{I}}{P_s}\Big)+e^{\frac{N_0B}{P_s\sigma_{ps}^2}}E_1\Big(\frac{N_0B}{P_s\sigma_{ps}^2}\Big)\Bigg)+E_1\Big(\frac{\mathcal{I}}{P_s\sigma_{sp}^2}\Big). \tag{32}$$

Finally, it can be observed that expectation $\mathbb{E}\{\mathcal{D}_2\}$ is the same with expecation $\mathbb{E}\{\mathcal{A}_2\}$, appearing in (10), thus we obtain

$$\mathbb{E}\{\mathcal{D}_2\}=\mathbb{E}\{\mathcal{A}_2\}. \tag{33}$$

C. Power policy at the secondary link under ZF

In this case, BS_p applies (as before) MRC BF with full power, P_p, while the BF vector applied at BS_s is the following

$$\mathbf{w}_{s,ZF}^{und}=\sqrt{P_{s,ZF}^{und}}\tilde{\mathbf{h}}_{ZF}^H, \tag{34}$$

where $\tilde{\mathbf{h}}_{ZF}$ is a unit norm vector belonging to the null space of vector $\mathbf{h}_{sp}$. Since we consider perfect estimation of this channel at BS_s, the interference created towards the PU will be equal to zero, thus, BS_s is free to transmit with full power, as a result

$$P_{s,ZF}^{und}=P_s. \tag{35}$$

In the following, an expression for the outage probability of PU will be given in closed form, as well as an expression describing the achievable ergodic capacity of the SU.

1) Outage probability of primary communication: As it has already been defined, an outage event occurs at the PU when the SINR of the PU is below threshold γ_0. Since, the use of a ZF BF vector at BS_s creates zero interference towards the PU, then the primary system will suffer from outages due to the deep fades of channel $\mathbf{h}_{pp}$. Hence, it is easy to show that the outage probability of PU is described by the following expression

$$\mathcal{P}_{out,ZF}^{und}=\mathcal{P}\Big\{\frac{P_p\|\mathbf{h}_{pp}\|^2}{N_0B}<\gamma_0\Big\}=\frac{\gamma\big(M,\frac{\gamma_0N_0B}{P_p\sigma_{pp}^2}\big)}{\Gamma(M)}. \tag{36}$$

2) Ergodic capacity of secondary communication: Applying the above described BF and power allocation policy, the expression that describes the achievable ergodic capacity of the SU is the one that follows

$$\mathbb{E}\{R_{s,ZF}^{und}\}=\mathcal{P}(\mathcal{H}_0)B\mathbb{E}\Big\{\underbrace{\log_2\Big(1+\frac{P_s|\mathbf{h}_{ss}\tilde{\mathbf{h}}_{ZF}^H|^2}{N_0B}\Big)}_{\mathcal{G}_1}\Big\}+\mathcal{P}(\mathcal{H}_1)B\mathbb{E}\Big\{\underbrace{\log_2\Big(1+\frac{P_s|\mathbf{h}_{ss}\tilde{\mathbf{h}}_{ZF}^H|^2}{N_0B+P_p|\mathbf{h}_{ps}\tilde{\mathbf{h}}_{pp}^H|^2}\Big)}_{\mathcal{G}_2}\Big\}. \tag{37}$$

a) Deriving expectation $\mathbb{E}\{\mathcal{G}_1\}$*:* Random variable $V_1 = |\mathbf{h}_{ss}\tilde{\mathbf{h}}_{ZF}^H|^2$ is exponentially distributed with PDF $f_{V_1}(v_1) = \frac{1}{\sigma_{ss}^2}e^{\frac{-v_1}{\sigma_{ss}^2}}$, thus, the computation of expectation $\mathbb{E}\{\mathcal{G}_1\}$ gives

$$\begin{aligned}\mathbb{E}\{\mathcal{G}_1\} &= \frac{1}{\ln(2)}\mathbb{E}\left\{\ln\left(1+\frac{P_sV_1}{N_0B}\right)\right\}\\ &= \frac{1}{\ln(2)}\int_0^\infty \ln\left(1+\frac{P_sv_1}{N_0B}\right)f_{V_1}(v_1)dv_1\\ &= \frac{1}{\ln(2)}e^{\frac{N_0B}{P_s\sigma_{ss}^2}}E_1\left(\frac{N_0B}{P_s\sigma_{ss}^2}\right),\end{aligned} \tag{38}$$

where integration by parts as well as [23, 3.352.4] were used for this derivation.

b) Deriving expectation $\mathbb{E}\{\mathcal{G}_2\}$*:* Working now on the derivation of $\mathbb{E}\{\mathcal{G}_2\}$, random variable $V_2 = Z_3 = |\mathbf{h}_{ps}\tilde{\mathbf{h}}_{pp}^H|^2$ is independent of V_1 and exponentially distributed with PDF $f_{V_2}(v_2) = \frac{1}{\sigma_{ps}^2}e^{\frac{-v_2}{\sigma_{ps}^2}}$, thus, one obtains

$$\mathbb{E}\{\mathcal{G}_2\} = \frac{1}{\ln(2)}\mathbb{E}\left\{\ln\left(1+\frac{P_sV_1}{N_0B+P_pV_2}\right)\right\}, \tag{39}$$

with

$$\begin{aligned}&\mathbb{E}\left\{\ln\left(1+\frac{P_sV_1}{N_0B+P_pV_2}\right)\right\}\\ &= \int_0^\infty f_{V_1}(v_1)\int_0^\infty \ln\left(1+\frac{P_sv_1}{N_0B+P_pv_2}\right)f_{V_2}(v_2)dv_2dv_1\\ &= \underbrace{\int_0^\infty f_{V_1}(v_1)\int_0^\infty \ln(N_0B+P_pv_2+P_sv_1)f_{V_2}(v_2)dv_2dv_1}_{\mathcal{M}_1}\\ &\quad - \underbrace{\int_0^\infty f_{V_1}(v_1)\int_0^\infty \ln(N_0B+P_pv_2)f_{V_2}(v_2)dv_2dv_1}_{\mathcal{M}_2}.\end{aligned} \tag{40}$$

The computation of term $\mathcal{M}_1$ gives, after using integration by parts and [23, 3.352.4] the following

$$\mathcal{M}_1 = \mathcal{M}_{1,1} + \mathcal{M}_{1,2}, \tag{41}$$

where, by using again [23, 3.352.4], we obtain

$$\mathcal{M}_{1,1} = \ln(N_0B) + e^{\frac{N_0B}{P_s\sigma_{ss}^2}}E_1\left(\frac{N_0B}{P_s\sigma_{ss}^2}\right). \tag{42}$$

Considering term $\mathcal{M}_{1,2}$, after a simple variable transformation we obtain the following expression

$$\mathcal{M}_{1,2} = \int_0^\infty e^{-w}e^{\frac{N_0B+P_s\sigma_{ss}^2w}{P_p\sigma_{ps}^2}}E_1\left(\frac{N_0B+P_s\sigma_{ss}^2w}{P_p\sigma_{ps}^2}\right), \tag{43}$$

which can be computed by exploiting Laguerre quadrature rules [19, 25.4.45].

Finally, the computation of term $\mathcal{M}_2$, gives, after integrating by parts and using [23, 3.352.4], the following expression

$$\mathcal{M}_2 = \ln(N_0B) + e^{\frac{N_0B}{P_p\sigma_{ps}^2}}E_1\left(\frac{N_0B}{P_p\sigma_{ps}^2}\right). \tag{44}$$

In the following section, the criteria for a fair comparison between the abovementioned CRN approaches are defined and the generic design parameters of each CRN approach are optimized in a rate-optimal sense for the SU.

V. Optimizing Generic Design Parameters of the CRN Approaches

In this section, the generic design parameters of each of the two examined CRN approaches will be optimized in the sense of maximizing the ergodic capacity of SU, subject to an outage probability constraint for primary communication, denoted by $\mathcal{P}_o$. In what follows, we start with the interweaved CRN approach.

A. Optimizing generic design parameters of an interweaved CRN

Concentrating on the interweaved approach, the optimization problem to be solved is the following

$$\begin{aligned}&(\epsilon^*,\tau^*) = \arg\max_{\epsilon,\tau}\ \mathbb{E}\{R_s^{int}\}\\ &s.t.\ \ \mathcal{P}_{out}^{int} = \mathcal{P}_o,\ \ 0\le\tau\le T,\ \ \epsilon\ge 0,\end{aligned} \tag{45}$$

where, considering the outage constraint, bound $\mathcal{P}_{d,B}$, presented in (6), is used. By analyzing the outage constraint of (45), one can express the energy detection threshold, ϵ, as a function of sensing time, τ, as follows

$$\epsilon = m_1\left(\frac{\delta}{\sqrt{\tau f_s}}+1\right), \tag{46}$$

where m_1 and δ are quantities equal to $P_p\sigma_{00}^2+N_0$ and $\mathcal{Q}^{-1}\left(\frac{\mathcal{P}_o-\mathcal{P}_1}{\mathcal{P}_2-\mathcal{P}_1}\right)$, respectively and $\mathcal{Q}^{-1}(\cdot)$ is the inverse of $\mathcal{Q}$-function. It should be noted that target outage probability, $\mathcal{P}_o$, is feasible for a specific interval of SINR QoS threshold, such that the argument of function $\mathcal{Q}^{-1}(\cdot)$ belongs to interval $(0,1)$. As a result, problem (45) will be expressed as follows

$$\begin{aligned}&(\epsilon^*,\tau^*) = \arg\max_{\epsilon,\tau}\ \mathbb{E}\{R_s^{int}\}\\ &s.t.\ \ \epsilon = m_1\left(\frac{\delta}{\sqrt{\tau f_s}}+1\right),\ \ 0\le\tau\le T,\ \ \epsilon\ge 0.\end{aligned} \tag{47}$$

With the aim of solving problem (47), the following proposition can be proved.

Proposition 3. Function $U(\tau) = \mathbb{E}\{R_s^{int}\}(\tau)$, which is obtained by substituting the outage probability constraint to the objective function of (47) is concave for $\tau\in[0,T]$.

Proof. See Appendix C. □

Capitalizing on Proposition 3, problem (47) can be solved by applying a gradient ascent method, which is described in Algorithm 1.

In what follows, the level of interference power received at the PU, $\mathcal{I}$, corresponding to the same target outage probability, $\mathcal{P}_o$, will be derived for the underlay CRN approach when MRC BF is applied at BS_s.

Algorithm 1 Optimizing ϵ and τ for a given $\mathcal{P}_o$

1 Initialization ($n = 0$). Select a $\tau_0 \in [0, T]$ and increase counter by one.
2 For the n-th iteration, compute value τ_n as follows

$$\tau_n = \tau_{n-1} + \lambda \frac{\partial U(\tau)}{\partial \tau}\bigg|_{\tau=\tau_{n-1}}, \quad (48)$$

where λ stands for the step of the algorithm.
3 Increase counter n by one and if $n > N_{max,1}$, where $N_{max,1}$ is a maximum number of iterations, stop, otherwise go to Step 2.
4 Having found τ^* compute the corresponding $\epsilon^* = m_1\left(\frac{\delta}{\sqrt{\tau^* f_s}} + 1\right)$.

B. Optimizing generic design parameters of an underlay CRN when MRC-based precoding is applied at BS_s

In this case, the interference temperature, $\mathcal{I}^*$, corresponding to the same target outage level, $\mathcal{P}_o$, can be found by setting $\mathcal{P}^{und}_{out,MRC} = \mathcal{P}_o$, which leads to equation $f(\mathcal{I}^*) = 0$. Function $f(\mathcal{I})$ has the expression that follows

$$f(\mathcal{I}) = \mathcal{P}^{und}_{out,MRC} - \mathcal{P}_o, \quad (49)$$

where the expression of $\mathcal{P}^{und}_{out,MRC}$ is given in (18).

As PU outage probability is monotonically increasing with $\mathcal{I}$, it is implied that there exists a single $\mathcal{I}^* \geq 0$ to search for and this can be accomplished by applying Newton's method as it is described in Algorithm 2.

Algorithm 2 Determine $\mathcal{I}^*$ for a given $\mathcal{P}_o$

1 Initialization ($n = 0$). Select an $\mathcal{I}_0 \geq 0$ and increase counter by one.
2 For the n-th iteration, compute value $\mathcal{I}_n$ as follows

$$\mathcal{I}_n = \mathcal{I}_{n-1} - f(\mathcal{I}_{n-1})\left(\frac{df(\mathcal{I})}{d\mathcal{I}}\bigg|_{\mathcal{I}=\mathcal{I}_{n-1}}\right)^{-1}. \quad (50)$$

3 Increase counter n by one and if $n > N_{max,2}$, where $N_{max,2}$ is a maximum number of iterations, stop, otherwise go to Step 2.

Considering an underlay CRN, where ZF BF is applied at BS_s, since zero interference will be created towards the PU, the throughput performance at the SU will be invariant of the outage probability constraint posed by the primary network.

In the section that follows, the throughput performance of the studied CRN approaches will be evaluated.

VI. Numerical Evaluation

In order to evaluate the performance of the examined CRN approaches under different conditions, extensive Monte Carlo (MC) simulations have been performed with the aim of confirming the validity of the theoretical expressions derived. More specifically, 5000 MAC frames were simulated. According to the scenario, the strengths of the involved channels are: $\sigma^2_{pp} = \sigma^2_{ss} = 10$ dB for the direct links, $\sigma^2_{ps} = \sigma^2_{sp} = 9$ dB for the cross-links and $\sigma^2_{00} = 6$ dB for the link between BS_p and BS_s, which is devoted to spectrum sensing. Moreover, we set B = 1Hz, f_s = 6MHz and T=100ms. Also, we consider unit noise variance in the system. In addition, the SINR level of the PU, γ_0, below which an outage occurs is chosen such that only a 10% rate loss, compared to the interference-free case, can be tolerated at the PU.

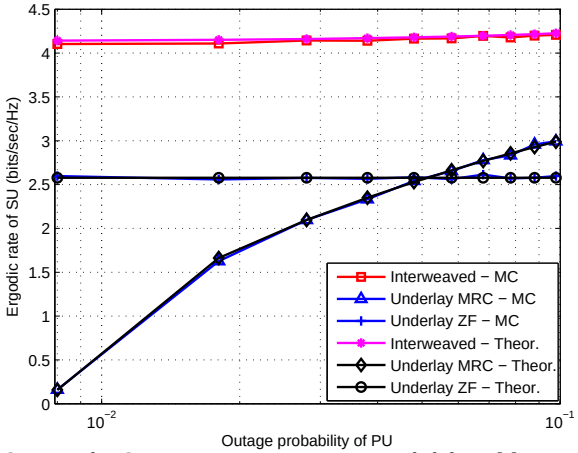

Fig. 3. Ergodic SU capacity vs. PU outage probability, M=4 antennas, $\mathcal{P}(\mathcal{H}_1) = 0.2$.

In Fig. 3, the ergodic rate of the SU, considering an interweaved CRN is illustrated as a function of the primary system's outage probability and compared with the ergodic rate achieved at the SU when the underlay approach (concerning both BF schemes) is adopted. Both MC and theoretical curves are depicted. In the examined scenario, the primary system is sporadically active with probability $\mathcal{P}(\mathcal{H}_1)$= 0.2 and the BSs are equipped with $M = 4$ antennas, each. The curves shown demonstrate a clear capacity gain to the benefit of the interweaved CRN approach for the whole examined interval of PU outage probability. However, the SU throughput in the underlay approach, when MRC precoding is applied at BS_s, is fastly increasing with the outage probability level, resulting to a reduced throughput gain in favour of the interweaved approach for relatively high outage probabilities of the PU. Also, considering the performance of the underlay approach, when ZF precoding is applied at BS_s, it is observed that it outperforms the MRC-based one for low PU outage probabilities, while this behavior changes for PU outage probabilities higher than 5%.

In Fig. 4, the achievable average rate of the SU, is depicted as a function of the outage probability of the PU, with the only difference lying in the fact that the primary system is characterized by a high activity profile ($\mathcal{P}(\mathcal{H}_1)$=0.8). One can observe that, for low target outage probabilities at the PU, the ZF-based underlay CRN approach, outperforms the other two, while, as the outage probability of PU increases, the MRC-based underlay approach starts to show a performance gain, first in comparison with the interweaved one (when $\mathcal{P}_o$ becomes higher than 2%) and then in comparison with the ZF-based underlay one (when $\mathcal{P}_o$ becomes higher than 5%).

The same performance metric is depicted in Fig. 5, as a function of primary system's activity profile when the target PU outage probability is 1% and for two different numbers

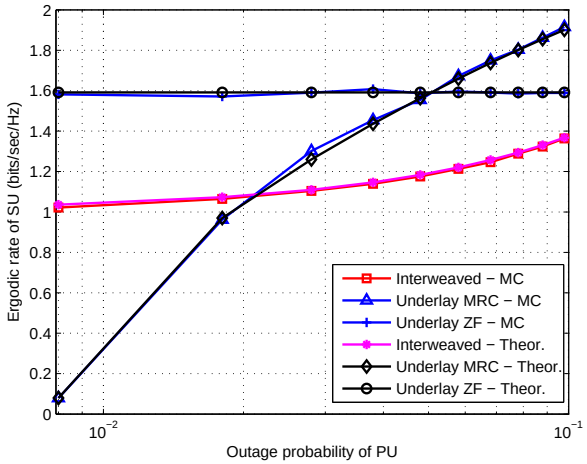

Fig. 4. Ergodic SU capacity vs. PU outage probability, M=4 antennas, $\mathcal{P}(\mathcal{H}_1) = 0.8$.

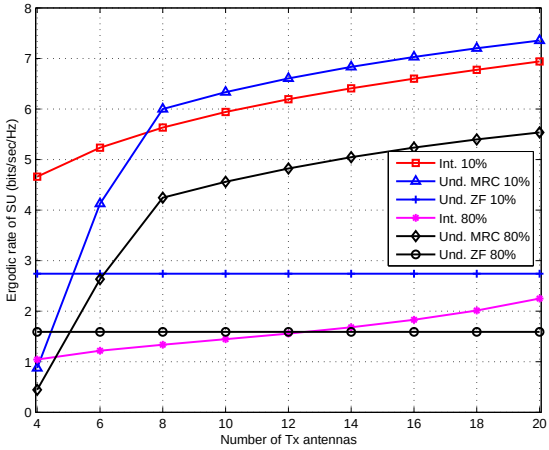

Fig. 6. Ergodic SU capacity vs. number of transmit antennas, M, target PU outage probability $\mathcal{P}_o = 0.01$.

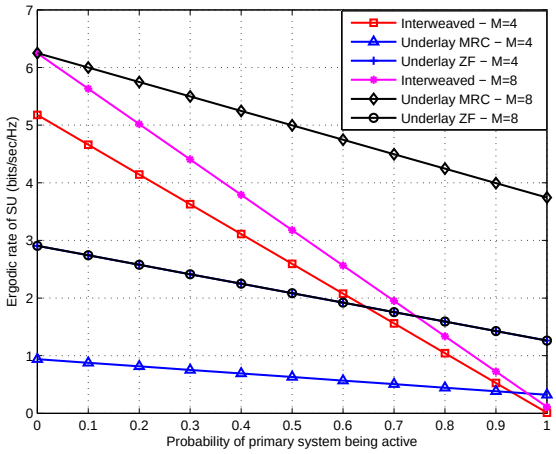

Fig. 5. Ergodic SU capacity vs. primary system's activity profile, target PU outage probability $\mathcal{P}_o = 0.01$.

of transmission antennas, $M = 4$ and $M = 8$, respectively. It can be observed that, regardless of the CRN approach followed, the ergodic capacity of the SU is a decreasing function of the activity rate of primary communication. This can be justified because as the primary network becomes highly active, the average interference (over time) received at the SU will be increasing. It is also worth noticing that the capacity gain achieved when the number of BS antennas is doubled is much larger in the MRC-based underlay approach, in comparison with the rate gain achieved in the interweaved approach, while this gain is zero for the ZF-based underlay approach. Also, it is interesting to mention that when $M = 8$, the performance of the underlay approach with MRC BF overcomes the performance of the interweaved one for all levels of primary activity.

In Fig. 6, the throughput performance is illustrated with reference to the number of transmitting antennas, M, for two different levels of primary activity, i.e., for primary systems that are transmitting for the 10% and 80% of the time. Also, the comparison is made for a common PU outage probability level of 1%. In this case, it is clear that an increase in the number of BS antennas enhances the ergodic capacity of the SU, with a large capacity gain appearing in favour of the underlay approach, as it was seen in Fig. 5.

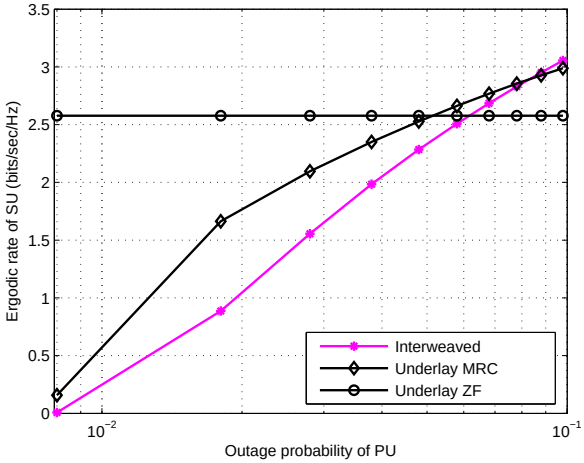

Fig. 7. Ergodic SU capacity vs. PU outage probability, $\mathcal{P}(\mathcal{H}_1) = 0.2$, weak $BS_p - BS_s$ link with strength $\sigma^2_{00} = -17$ dB.

Moreover, it can be seen that the number of BS antennas over which the MRC-based underlay approach outperforms the interweaved one in terms of ergodic SU capacity, depends on the activity profile of the primary network. More concretely, this change occurs when $M = 5$ antennas for a highly active primary network, whereas it is observed when $M = 8$ antennas for a primary network characterized by low activity.

Finally, in Fig. 7 the same metric is depicted as a function of the outage probability of the PU, when $\mathcal{P}(\mathcal{H}_1)$= 0.2, with the difference that channel $\mathbf{h}_{00}$, is much weaker than before ($\sigma^2_{00} = -17$ dB). As one would expect, the throughput performance of the interweaved approach is much more degraded in comparison with the one shown in Fig. 3. This occurs because as the channel useful for spectrum sensing becomes weaker, the secondary transmitter spends a considerable amount of secondary communication resources towards sensing, which leads to a degraded ergodic rate at the SU.

VII. Conclusions

In this paper, the interweaved CRN approach was examined and compared with the underlay CRN approach in terms of the ergodic throughput of the SU for a common PU outage level. Expressions for the ergodic capacity of the SU as well as for the outage probability of primary communication, were derived for both approaches and it was shown that the performance comparison results are driven by a set of key system parameters which are: (a) the activity profile of the primary system, (b) the number of transmit antennas, as well as (c) the quality of the sensed channel in the interweaved CRN approach.

Appendix A
Proof of Proposition 1

The outage probability of PU, considering an interweaved CRN, is described by the following expression

$$\mathcal{P}_{out}^{int} = \mathcal{P}_{out,1} + \mathcal{P}_{out,2}, \tag{51}$$

where for probability $\mathcal{P}_{out,1}$ we have

$$\begin{aligned}\mathcal{P}_{out,1} &= (1-\mathcal{P}_d)\mathcal{P}\left\{\frac{|\mathbf{h}_{pp}\mathbf{w}_p|^2}{N_0B+|\mathbf{h}_{sp}\mathbf{w}_s^{int}|^2}<\gamma_0\right\}\\ &= (1-\mathcal{P}_d)\mathcal{P}\left\{P_p\|\mathbf{h}_{pp}\|^2-\gamma_0P_s|\mathbf{h}_{sp}\tilde{\mathbf{h}}_{ss}^H|^2<\gamma_0N_0B\right\}\\ &= (1-\mathcal{P}_d)\mathcal{P}\big\{X_1-X_2<\gamma_0N_0B\big\}.\end{aligned} \tag{52}$$

Random variable $X_1 = P_p\|\mathbf{h}_{pp}\|^2$ is gamma distributed with probability density function (PDF): $f_{X_1}(x_1) = \frac{x_1^{M-1}e^{-\frac{x_1}{\lambda_{X_1}}}}{\Gamma(M)\lambda_{X_1}^M}$, where $\lambda_{X_1} = P_p\sigma_{pp}^2$. Also, random variable $X_2 = \gamma_0P_s|\mathbf{h}_{sp}\tilde{\mathbf{h}}_{ss}^H|^2$ is exponentially distributed with PDF $f_{X_2}(x_2) = \frac{1}{\lambda_{X_2}}e^{-\frac{x_2}{\lambda_{X_2}}}$, where $\lambda_{X_2} = \gamma_0P_s\sigma_{sp}^2$. As X_1 and X_2 are independent, their joint PDF $f_{X_1,X_2}(x_1,x_2)$ will be the product of the two marginal PDFs. Consequently, the computation of probability $\mathcal{P}_{out,1}$ gives

$$\mathcal{P}_{out,1} = (1-\mathcal{P}_d)\int_0^\infty\int_0^{x_2+\gamma_0N_0B} f_{X_1,X_2}(x_1,x_2)dx_1dx_2. \tag{53}$$

The double integral appearing in (53) can be computed by applying [23, 3.351.1] and [23, 3.351.2] for the inner and the resulting integral, respectively. As a result, we obtain

$$\mathcal{P}_{out,1} = (1-\mathcal{P}_d)\mathcal{P}_1, \tag{54}$$

where probability $\mathcal{P}_1$ is given by (9a).

Probability $\mathcal{P}_{out,2}$ is given by the following expression

$$\begin{aligned}\mathcal{P}_{out,2} &= \mathcal{P}_d\mathcal{P}\left\{\frac{P_p\|\mathbf{h}_{pp}\|^2}{N_0B}<\gamma_0\right\}\\ &= \mathcal{P}_d\mathcal{P}\big\{X_1<\gamma_0N_0B\big\} = \mathcal{P}_d\mathcal{P}_2,\end{aligned} \tag{55}$$

where $\mathcal{P}_2$ is given by (9b) and [23, 3.351.1] was used for the derivation. Substituting (54) and (55) to (51) we yield (8), thus Proposition 1 is proved.

Appendix B
Proof of Proposition 2

Taking into consideration the followed BF and truncated power allocation policy, one will obtain the following expression for the outage probability of primary communication

$$\begin{aligned}\mathcal{P}_{out,MRC}^{und} &= \mathcal{P}\left\{\frac{\mathcal{I}}{|\mathbf{h}_{sp}\tilde{\mathbf{h}}_{ss}^H|^2}<P_s\right\}\mathcal{P}\left\{\frac{P_p\|\mathbf{h}_{pp}\|^2}{N_0B+\mathcal{I}}<\gamma_0\right\}\\ &+\mathcal{P}\left\{\frac{\mathcal{I}}{|\mathbf{h}_{sp}\tilde{\mathbf{h}}_{ss}^H|^2}\geq P_s,\quad \frac{P_p\|\mathbf{h}_{pp}\|^2}{N_0B+P_s|\mathbf{h}_{sp}\tilde{\mathbf{h}}_{ss}^H|^2}<\gamma_0\right\}.\end{aligned} \tag{56}$$

Capitalizing on the known distribution of random variables $\|\mathbf{h}_{pp}\|^2$ and $|\mathbf{h}_{sp}\tilde{\mathbf{h}}_{ss}^H|^2$, the probabilities appearing in the first term of (56) can be found in closed form, giving

$$\mathcal{P}\left\{\frac{\mathcal{I}}{|\mathbf{h}_{sp}\tilde{\mathbf{h}}_{ss}^H|^2}<P_s\right\} = e^{-\frac{\mathcal{I}}{P_s\sigma_{sp}^2}}, \tag{57}$$

which is obtained by applying integration by parts and

$$\mathcal{P}\left\{\frac{P_p\|\mathbf{h}_{pp}\|^2}{N_0B+\mathcal{I}}<\gamma_0\right\} = \frac{\gamma\big(M,\frac{\gamma_0(N_0B+\mathcal{I})}{P_p\sigma_{pp}^2}\big)}{\Gamma(M)}, \tag{58}$$

which is derived by applying [23, 3.351.1]. Focusing on the joint probability appearing in the second term of (56), we obtain

$$\begin{aligned}&\mathcal{P}\left\{\frac{\mathcal{I}}{|\mathbf{h}_{sp}\tilde{\mathbf{h}}_{ss}^H|^2}\geq P_s,\quad \frac{P_p\|\mathbf{h}_{pp}\|^2}{N_0B+P_s|\mathbf{h}_{sp}\tilde{\mathbf{h}}_{ss}^H|^2}<\gamma_0\right\}\\ &= \mathcal{P}\left\{|\mathbf{h}_{sp}\tilde{\mathbf{h}}_{ss}^H|^2\leq\frac{\mathcal{I}}{P_s},P_p\|\mathbf{h}_{pp}\|^2-\gamma_0P_s|\mathbf{h}_{sp}\tilde{\mathbf{h}}_{ss}^H|^2<\gamma_0N_0B\right\}.\end{aligned} \tag{59}$$

By applying a bivariate transformation, it is easy to show that the joint PDF of random variables $W_1 = |\mathbf{h}_{sp}\tilde{\mathbf{h}}_{ss}^H|^2$ and $W_2 = P_p\|\mathbf{h}_{pp}\|^2-\gamma_0P_s|\mathbf{h}_{sp}\tilde{\mathbf{h}}_{ss}^H|^2$ is

$$\begin{aligned}f_{W_1,W_2}(w_1,w_2) = &\frac{e^{-w_1\left(\frac{1}{\sigma_{sp}^2}+\frac{P_s\gamma_0}{P_p\sigma_{pp}^2}\right)}}{P_p\Gamma(M)\sigma_{sp}^2(\sigma_{pp}^2)^M}\times\\ &\left(\frac{\gamma_0P_s}{P_p}w_1+\frac{1}{P_p}w_2\right)^{M-1}e^{\frac{-w_2}{P_p\sigma_{pp}^2}}.\end{aligned} \tag{60}$$

As a result, the probability to be derived is the following

$$\mathcal{P}\left\{W_1\leq\frac{\mathcal{I}}{P_s},W_2<\gamma_0N_0B\right\} = \int_0^{\frac{\mathcal{I}}{P_s}}\int_{-P_s\gamma_0w_1}^{\gamma_0N_0B} f_{W_1,W_2}(w_1,w_2)dw_2dw_1, \tag{61}$$

from which a closed form expression can be obtained. After some mathematical manipulations and by applying [23, 3.351.1] and [23, 3.351.2], one can conclude to the following expression

$$\mathcal{P}\Big\{W_1 \le \frac{\mathcal{I}}{P_s}, W_2 < \gamma_0 N_0 B\Big\} = \frac{\gamma\big(M, \frac{\gamma_0 N_0 B}{P_p \sigma_{pp}^2}\big)}{\Gamma(M)} - e^{\frac{-\mathcal{I}}{P_s \sigma_{sp}^2}} \frac{\gamma\big(M, \frac{\gamma_0(N_0 B+\mathcal{I})}{P_p \sigma_{pp}^2}\big)}{\Gamma(M)} + \frac{e^{\frac{N_0 B}{P_s \sigma_{sp}^2}}}{\Gamma(M)} \Big(\frac{P_p \sigma_{pp}^2}{\gamma_0 P_s \sigma_{sp}^2} + 1\Big)^{-M} \times \Big(\Gamma\Big(M, \frac{N_0 B}{P_s \sigma_{sp}^2} + \frac{\gamma_0 N_0 B}{P_p \sigma_{pp}^2}\Big) - \Gamma\Big(M, \frac{N_0 B + \mathcal{I}}{P_s \sigma_{sp}^2} + \frac{\gamma_0(N_0 B+\mathcal{I})}{P_p \sigma_{pp}^2}\Big)\Big). \tag{62}$$

After substituting (57), (58) and (62) to (56), expression (18) will be obtained. As a result, Proposition 2 is proved.

APPENDIX C
PROOF OF PROPOSITION 3

The objective function of (47) can be expressed as

$$\begin{aligned} U(\tau,\epsilon) = \mathbb{E}\{R_s^{int}(\tau,\epsilon)\} &= \frac{(T-\tau)}{T}\Big\{\underbrace{\mathcal{P}(\mathcal{H}_0)B\mathbb{E}\{\mathcal{A}_1\}}_{\alpha}(1-\mathcal{P}_{fa}) \\ &\quad + \underbrace{\mathcal{P}(\mathcal{H}_1)B\mathbb{E}\{\mathcal{A}_2\}}_{\beta}(1-\mathcal{P}_{d,B})\Big\} \\ &\overset{(4),(6)}{=} \frac{(T-\tau)}{T}\Big\{\alpha\Big(1-\mathcal{Q}\Big(\sqrt{\tau f_s}\Big(\frac{\epsilon-N_0}{N_0}\Big)\Big)\Big) \\ &\quad + \beta\Big(1-\mathcal{Q}\Big(\sqrt{\tau f_s}\Big(\frac{\epsilon-m_1}{m_1}\Big)\Big)\Big)\Big\}. \end{aligned} \tag{63}$$

By substituting the equality constraint of (47) to (63), the following one variable objective function can be obtained

$$U(\tau) = \frac{(T-\tau)}{T}\big(\alpha\big(1-\mathcal{Q}(t_1\sqrt{\tau f_s}+t_2)\big) + \beta(1-\mathcal{Q}(\delta))\big), \tag{64}$$

where $t_1 = \frac{P_p\sigma_{00}^2}{N_0}$ and $t_2 = \frac{\delta m_1}{N_0}$. Taking the first derivative of (64) with respect to τ, we obtain

$$\begin{aligned} \frac{\partial U(\tau)}{\partial \tau} &= -\frac{1}{T}\alpha\big(1-\mathcal{Q}(t_1\sqrt{\tau f_s}+t_2)\big) \\ &\quad + \frac{(T-\tau)\alpha t_1 f_s}{2T\sqrt{2\pi}\sqrt{\tau f_s}} e^{-\frac{(t_1\sqrt{\tau f_s}+t_2)^2}{2}} - \frac{1}{T}\beta\big(1-\mathcal{Q}(\delta)\big). \end{aligned} \tag{65}$$

Taking the derivative of (65) we obtain

$$\begin{aligned} \frac{\partial^2 U(\tau)}{\partial \tau^2} &= -e^{-\frac{(t_1\sqrt{\tau f_s}+t_2)^2}{2}}\Big(\frac{\alpha t_1 f_s}{T\sqrt{2\pi}\sqrt{\tau f_s}} \\ &\quad + \frac{(T-\tau)\alpha t_1 f_s^2}{4T\sqrt{2\pi}(\tau f_s)^{\frac{3}{2}}} + \frac{(T-\tau)\alpha t_1^2 f_s^2 (t_1\sqrt{\tau f_s}+t_2)}{4T\sqrt{2\pi}(\tau f_s)}\Big) \\ &\quad \le 0, \end{aligned} \tag{66}$$

thus, according to the second derivative criterion, function $U(\tau, \epsilon(\tau))$ is concave for every $\tau \in [0, T]$, which completes the proof.

REFERENCES

[1] Federal Communications Commission, "Spectrum policy task force report, FCC 02-155," 2002.

[2] J. Mitola and G. Q. Maguire Jr, "Cognitive radio: making software radios more personal," *IEEE, Personal Communications*, vol. 6, no. 4, pp. 13–18, Aug. 1999.

[3] S. Haykin, "Cognitive radio: brain-empowered wireless communications," *IEEE Journal on Selected Areas in Communications*, vol. 23, no. 2, pp. 201–220, Feb. 2005.

[4] E. Biglieri, A. J. Goldsmith, L. J. Greenstein, N. Mandayam, and H. V. Poor, *Principles of Cognitive Radio*. Cambridge University Press, 2012.

[5] A. Goldsmith, S. Jafar, I. Maric, and S. Srinivasa, "Breaking spectrum gridlock with cognitive radios: An information theoretic perspective," *Proceedings of the IEEE*, vol. 97, no. 5, pp. 894–914, May 2009.

[6] S. Srinivasa and S. Jafar, "The throughput potential of cognitive radio: A theoretical perspective," in *Fortieth Asilomar Conference on Signals, Systems and Computers, 2006. ACSSC '06*, Oct. 2006, pp. 221–225.

[7] A. Giorgetti, M. Varrella, and M. Chiani, "Analysis and performance comparison of different cognitive radio algorithms," in *Second International Workshop on Cognitive Radio and Advanced Spectrum Management, 2009. CogART 2009.*, May 2009, pp. 127–131.

[8] M. Khoshkholgh, K. Navaie, and H. Yanikomeroglu, "Access strategies for spectrum sharing in fading environment: Overlay, underlay, and mixed," *IEEE Transactions on Mobile Computing*, vol. 9, no. 12, pp. 1780–1793, Dec. 2010.

[9] X. Kang, Y.-C. Liang, H. Garg, and L. Zhang, "Sensing-based spectrum sharing in cognitive radio networks," *IEEE Transactions on Vehicular Technology*, vol. 58, no. 8, pp. 4649–4654, Oct. 2009.

[10] Y. Wang, P. Ren, F. Gao, and Z. Su, "A hybrid underlay/overlay transmission mode for cognitive radio networks with statistical quality-of-service provisioning," *IEEE Transactions on Wireless Communications*, vol. PP, no. 99, pp. 1–17, Mar. 2014.

[11] A. Ghasemi and E. Sousa, "Fundamental limits of spectrum-sharing in fading environments," *IEEE Transactions on Wireless Communications*, vol. 6, no. 2, pp. 649–658, Feb. 2007.

[12] C.-X. Wang, X. Hong, H.-H. Chen, and J. Thompson, "On capacity of cognitive radio networks with average interference power constraints," *IEEE Transactions on Wireless Communications*, vol. 8, no. 4, pp. 1620–1625, Apr. 2009.

[13] L. Musavian and S. Aissa, "Ergodic and outage capacities of spectrum-sharing systems in fading channels," in *IEEE Global Telecommunications Conference, 2007. GLOBECOM '07*, Nov. 2007, pp. 3327–3331.

[14] L. Sboui, Z. Rezki, and M.-S. Alouini, "A unified framework for the ergodic capacity of spectrum sharing cognitive radio systems," *IEEE Transactions on Wireless Communications*, vol. 12, no. 2, pp. 877–887, Feb. 2013.

[15] H. Suraweera, P. Smith, and M. Shafi, "Capacity limits and performance analysis of cognitive radio with imperfect channel knowledge," *IEEE Transactions on Vehicular Technology*, vol. 59, no. 4, pp. 1811–1822, May 2010.

[16] S. Stotas and A. Nallanathan, "On the outage capacity of sensing-enhanced spectrum sharing cognitive radio systems in fading channels," *IEEE Transactions on Communications*, vol. 59, no. 10, pp. 2871–2882, Oct. 2011.

[17] B. Makki and T. Eriksson, "On the ergodic achievable rates of spectrum sharing networks with finite backlogged primary users and an interference indicator signal," *IEEE Transactions on Wireless Communications*, vol. 11, no. 9, pp. 3079–3089, Sep. 2012.

[18] M. Filippou, D. Gesbert, and G. Ropokis, "Underlay versus interweaved cognitive radio networks: a performance comparison study," in *International Conference on Cognitive Radio Oriented Wireless Networks (CROWNCOM 2014) - accepted*, 2014.

[19] M. Abramowitz and I. A. Stegun, *Handbook of mathematical functions*. Dover publications, 1965.

[20] M. K. Simon and M.-S. Alouini, *Digital communication over fading channels*. John Wiley & Sons, 2005, vol. 95.

[21] I. F. Akyildiz, W.-Y. Lee, M. C. Vuran, and S. Mohanty, "Next generation/dynamic spectrum access/cognitive radio wireless networks: a survey," *Computer Networks*, vol. 50, no. 13, pp. 2127–2159, Sep. 2006.

[22] Y.-C. Liang, Y. Zeng, E. Peh, and A. T. Hoang, "Sensing-throughput tradeoff for cognitive radio networks," *IEEE Transactions on Wireless Communications*, vol. 7, no. 4, pp. 1326–1337, Apr. 2008.

[23] I. S. Gradshteyn and I. M. Ryzhik, *Table of integrals, series, and products*, 7th ed. Elsevier/Academic Press, Amsterdam, 2007.

[24] D. Tse, *Fundamentals of wireless communication*. Cambridge university press, 2005.